ANALYSIS OF LOAD TRANSFER BEHAVIOUR AND DETERMINATION OF INTERFACIAL SHEAR STRENGTH IN SINGLE-FIBRE-REINFORCED TITANIUM ALLOYS

Theodore E. Matikas

Department of Materials Science and Engineering, University of Ioannina,
University Campus, 45110 Ioannina, Greece
E-mail: matikas@otenet.gr

Received 16 July 2007; accepted 21 September 2007

ABSTRACT

The effect of interfaces on load sharing behaviour has been evaluated by performing single-fibre fragmentation (SFF) experiments and analysis of titanium matrix composites at ambient and elevated temperatures. Fibre breaks were monitored by acoustic emission sensors, and the break locations were determined in-situ by an innovative ultrasonic non-destructive evaluation technique. Data analysis of SFF testing was performed using the Kelly-Tyson model. The length of fibre fragments and distribution were determined using innovative nondestructive technique. This study demonstrates that composite processing conditions can significantly affect the nature of the fibre/matrix interface and the resulting fragmentation behaviour of the fibre. Further, thermal micro-residual stresses, generated during the fabrication process and in-service due to the difference in thermo-mechanical characteristics of the model composite's constituents, play a major role influencing the interfacial shear stress transfer behaviour in single-fibre titanium matrix composites.

***Keywords*:** Fibre/matrix interface, fibre fragmentation, titanium, metal matrix composites

1. INTRODUCTION

One of the most important mechanisms in fibre-reinforced composites for application in high stress primary structures is the stress transfer between the fibre and matrix across the interface when the composite is subjected to various loading conditions [1-7]. During the past several decades, a significant effort has been put into understanding the stress transfer in various forms of micro-composite tests as a means of evaluating the bond quality at the fibre-matrix interface region.

Cox [8], first considered a shear-lag model where an elastic fibre is embedded in an elastic matrix which is subjected to uniaxial tension. Perfect bonding is assumed at the interface between the fibre and the matrix, and the Poisson contraction in the lateral direction is the same in the fibre and matrix. Later, Dow [9] modified Cox's model, assuming that the matrix axial displacement is not constant and there is no matrix present at the end of the fibre. Rosen [10] further refined the models by Cox and Dow considering that the matrix encapsulating the fibre is in turn surrounded by a material having the average properties of the composite. Amirbayat and Hearle [11] considered elastic-plastic deformations with the assumption of a constant interfacial shear stress in regions where the interface had failed. Molliex et al. [12] studied fragmentation in SCS-2 SiC fibre-reinforced aluminum alloy composites and concluded that interfacial stress transfer in these metal matrix composites is limited by the plastic deformation of the matrix alloy. Clough et al. [13] and Houpert et al. [14] conducted single fibre fragmentation (SFF) tests on SiC fibre-reinforced single crystal Al and Al_2O_3 fibre-reinforced Cu matrix composites, respectively, and analyzed the results in terms of the load drops corresponding to fibre fragmentation.

Early work of Kelly and Tyson [15] suggested that reinforcement effect would occur when the volume fraction of fibres is above a critical value and multiple fractures or fragmentation of fibres would take place when the fibre volume fraction is below a certain minimum value. On this basis, the study of fibre fragmentation requires testing of composite specimens with a relatively low volume fraction of fibres. The test which is most commonly performed is the single fibre fragmentation test in which a dog bone-shaped specimen consisting of an isolated fibre embedded in matrix material is loaded in tension along the fibre axis to an elongation greater than that

required to fracture the fibres. The traction stress, applied externally, is transferred to the fibre by means of a shear stress across the interface. The tensile stress in the fibre increases from nearly zero at the fibre ends to a maximum value, limited by the breaking stress of the fibre. As the applied strain increases this limit is reached causing the fibre to break at its weakest point, thereby producing many smaller fragments and the fibre stress decays to zero near these breaks. If it is not long enough, the fibre will not break, since the generated tensile stress at the centre section is below the nominal uniform stress. The fibre length for which the generated tensile stress reaches a value of the breaking strength of the fibre exactly at the midpoint of the length is called the "critical length", L_c. With continued loading, fragments longer than the critical length will experience an increasing, uniform stress only over their centre sections, which are susceptible to further breakage (Fig. 1). Using shear-lag analysis, Kelly and Tyson [15] have related the critical length L_c to the

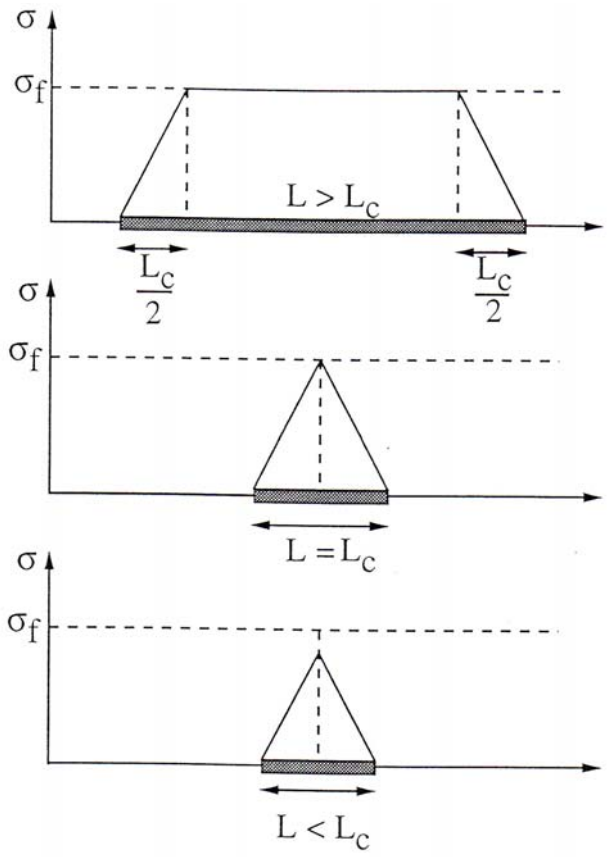

Fig. 1: Schematic illustration indicating the stress profile in embedded fibre segments in a single fibre composite during fragmentation test, assuming constant fibre strength (σ_f).

yield stress of the matrix at the interface τ_y through a force balance around the embedded fibre. They assumed that the shear stress at the interface is constant and equal to the yield strength of the matrix or the "resistance" of the interface and obtained the following equation for the critical length:

$$\tau_y = \frac{\sigma_f \, d}{2 \, L_c} \qquad (1)$$

where τ_y is the shear strength of the interface, σ_f is the average breaking strength of the fibre, and d is the fibre diameter. This relationship, sometimes called the Kelly-Tyson equation, suggests that the lengths of fibre fragments are a measure of the ability of the fibre/matrix interface to transmit the imposed stresses from the matrix to the fibre. The relation between the distribution of fragment lengths and the ability of the interface to transmit stresses depends on the mechanism of stress transfer between matrix and fibre. In practice, however, the SFF test usually results in a wide distribution of fragment lengths since the strength of fibre fragments depends on their length [16, 17]. Therefore, the determination of interfacial shear strength using fragment length data is more complicated as discussed elsewhere [16 19]. In spite of these complexities, the SFF test has been widely applied since it allows simulation of the interfacial load transfer occurring in real composite specimens subjected to longitudinal tensile loading and closely approximates the chemical and thermo mechanical effects present at the interfaces of real composites. It should be noted that the fibre fragmentation characteristics in metal matrix and the resulted interfacial shear strength are largely influenced by the friction arising from thermal residual stresses present in the composite [20].

The importance of residual stresses cannot be overemphasized in composites technology because the combination of dissimilar materials in a composite creates inevitably an interface across which micro-residual stresses are generated during fabrication and in service due to the difference in thermo-mechanical characteristics. It is well established that these residual stresses have a significant effect on the composite properties. For example, due to the presence of residual stresses, it is almost never

possible to achieve the maximum elastic response of the composites. In addition, yield stress and fracture toughness of the composites are significantly affected by residual stresses. This process-induced stress is essentially thermal in nature and is caused by a significant difference in the coefficients of thermal expansion (CTE) of the fibre and the matrix and the large temperature differential of the cooling process. When the composite is fabricated at high temperatures both the fibre and the matrix are relatively stress-free and when they are cooled down to ambient temperature residual stresses are induced due to thermo-mechanical mismatch. The problem is more predominant in metal matrix composites than in polymeric matrix composites, due to the higher processing temperatures and higher stiffness of the matrix. Additional thermal stresses may be created if the coefficients of thermal conductivity and thermal capacity of the constituents are different or the mechanical and thermal properties of the materials are functions of temperature. These phenomena will create thermal gradients inside the material, which eventually generate thermal stresses. The generation of thermal residual stresses in SiC/Ti-6Al-4V composite when cooling from a high manufacturing temperature was investigated by Nimmer et al. [21], where 3-D FEM elements were used to model the unit cell of the rectangle fibre array pattern. Furthermore, many analytical [22-26] and experimental [27-30] studies are reported in the literature on residual thermal stresses.

This paper deals with the influence of the composite's fabrication process on the nature of the fibre/matrix interface and the resulting load transfer behaviour from matrix to fibre. The load transfer behaviour was studied by fibre fragmentation testing, where fibre break locations were obtained using advanced ultrasonic non-destructive evaluation techniques. Further, the interfacial shear strength in titanium matrix composites was determined, taking into account the effect of thermal micro-residual stresses, which are present in the composite due to processing conditions.

2. MATERIALS AND METALLOGRAPHIC EXAMINATION

Two different titanium alloys were used as a matrix material in this study; Ti-6Al-4V wt.% and Ti-14Al-2lNb wt.% (or Ti-24Al-11Nb at.%). The single fibre composite samples were fabricated by diffusion bonding of a Textron (Textron Specialty Material Division, Lowell, MA) SCS-6 silicon carbide fibre placed between the matrix alloy sheets using: (i) A two-stage process involving vacuum hot pressing at 925°C under 5.5 MPa pressure for 30 min followed by hot isostatic pressing at 985°C under 100 MPa pressure for 2 hours, then cooled to room temperature. (ii) A single-stage consolidation process involving vacuum hot pressing at 954°C under a pressure of 9.2 MPa for 30 min.

The SCS-6 monofilament consists essentially of a silicon carbide sheath with an outer diameter of 142 μm surrounding a pyrolytic graphite-coated carbon core. The fibre has an approximately 3 μm thick coating consisting of SiC particles embedded in pyrolytic carbon. The consolidated composite panels were machined into 1.5 mm thick dog-bone type tensile specimens with 19.0 mm x 6.4 mm gage sections. The properties of the composite constituents used in this study are shown in Table 1.

Table 1: CTE and Young's modulus of matrix and fibre materials.

Material	Linear CTE (x 10^{-6} °C)	E (GPa)
Ti-6Al-4V	9,7	114
Ti-14Al-21Nb	9,9	112
SCS-6 fibre	6,5	393

The extent of fibre/matrix reaction in the composite samples was characterized by metallographic examination of their cross sections. The Ti 6Al 4V/SCS 6 system fabricated by the two-stage process exhibited a significant reaction zone with a very rough interface, which was produced due to preferential reaction between the β - phase of the matrix alloy and the carbon rich coating layers of the fibre (Fig. 2a). Much of the outer, carbon rich layer of the SCS 6 fibre coating was consumed by this reaction, and a part of its inner, carbon rich layer, was also attacked by the matrix at several locations along the fibre. In contrast, the Ti-14Al 2lNb/SCS 6 composite fabri-

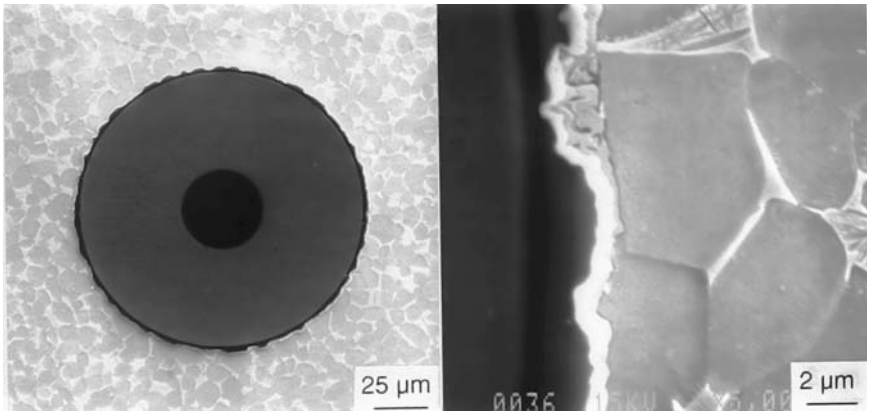

(a)

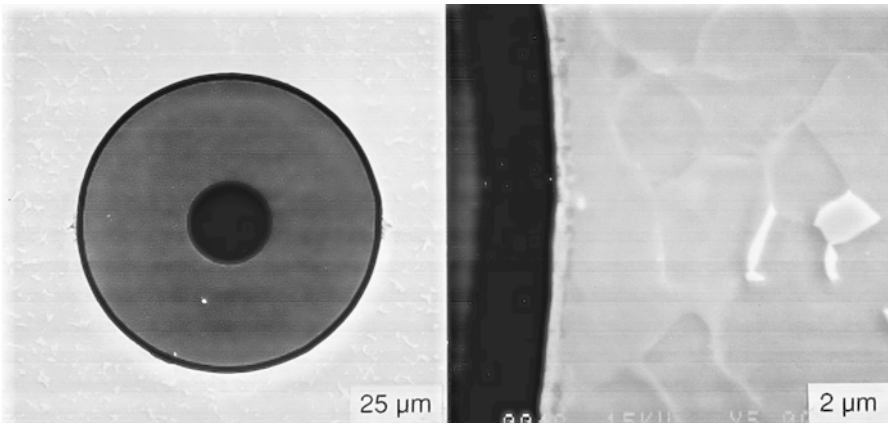

(b)

Fig. 2: SEM micrographs showing the fibre-matrix interface, and detail of the interfacial region, in single fibre composites fabricated by the two-stage process: (a) Ti-6Al-4V/SCS-6 and (b) Ti-14Al-21Nb/SCS-6.

cated by the two-stage process showed a narrower and smoother interfacial reaction zone (Fig. 2b). However, this composite showed a wide region of the matrix adjacent to the fibre was devoid of the β-phase. The formation of the reduced reaction zone consisting of complex carbides and silicides along with the presence of a wide β-depleted region in this composite. Ti 6Al 4V/SCS 6 composites fabricated by the single-stage process showed a significantly smoother fibre-matrix interface that those fabricated by the two-stage process. Furthermore, the single-stage process was inadequate for achieving full consolidation of the Ti 14Al 2lNb/SCS 6 composite.

3. MECHANICAL TESTING

Tensile tests were conducted at ambient and elevated temperatures using a nominal strain rate of $2x10^{-4}$ s^{-1} for Ti-6Al-4V/SCS-6 and $1x10^{-4}$ s^{-1} for Ti-14Al-2lNb/SCS-6 specimens. Tensile loading was continued until fracture of the specimen. Acoustic emission activity was monitored during the tensile tests using a broadband resonant transducer with a nominal centre frequency of 250 kHz, which was coupled via high vacuum grease to the flat gage section of the samples. The thermally induced axial residual strain in the fibre was also quantified in a few composite samples by dissolving a portion of the matrix surrounding the fibre and measuring the resulting fibre protrusion [31].

4. EVALUATION OF FIBRE FRAGMENTATION BEHAVIOUR

Based on the acoustic emission characteristics of fibre fractures, it was observed that fragmentation attains saturation in the Ti-6Al-4V/SCS-6 specimens due to the severity of fibre-matrix reaction and interface roughness causing extensive fracture. On the other hand, Ti-14Al-2lNb/SCS-6 composites exhibited longer fragments and did not attain saturation of fibre fragmentation. Total number of all acoustic emission signals was found to be equal to the total number of fractures.

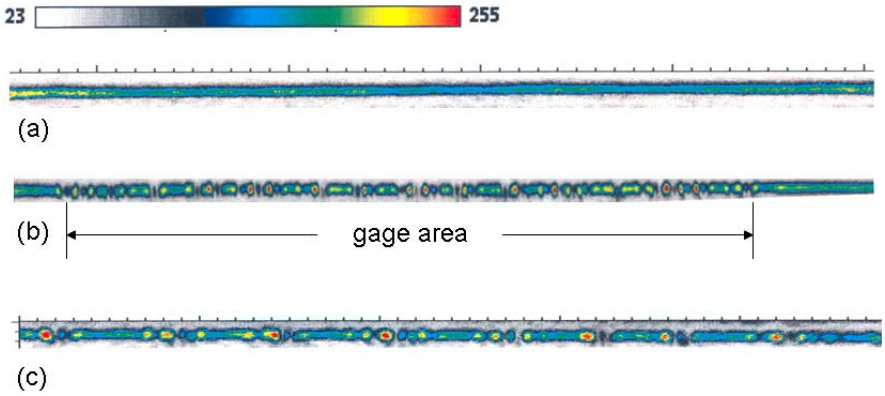

Fig. 3: Ultrasonic images from a fully consolidated, single fibre composite using the ultrasonic shear-wave back reflection technique: (a) As-fabricated Ti-6Al-4V/SCS-6, (b) Tensile tested Ti-6Al-4V/SCS-6 at room temperature, and (c) Tensile tested Ti-14Al-21Nb/SCS-6 at room temperature.

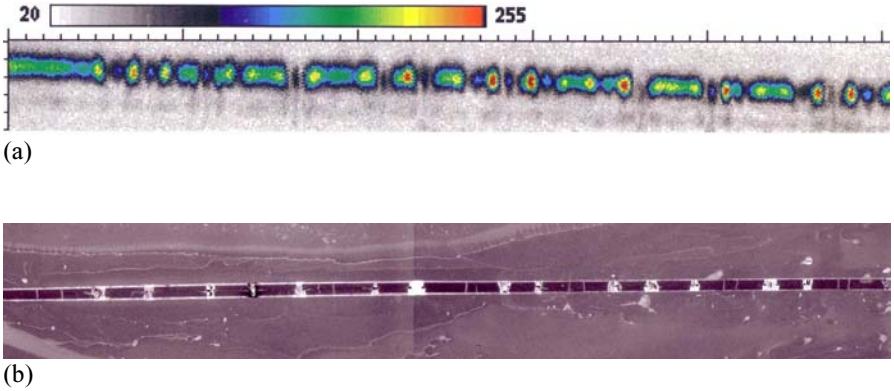

Fig. 4: Single fibre, Ti-6Al-4V/SCS-6 composite, tensile tested at room temperature: (a) Ultrasonic image using the shear-wave back reflection technique showing fibre fragments, and (b) SEM micrograph of the same sample.

The number and length of the fragments were measured using ultrasonic imaging. The embedded fibre in the composites was ultrasonically imaged using the shear-wave back reflection (SBR) technique [32]. A focused ultrasonic transducer was used in the pulse-echo mode to propagate a 25 MHz in frequency ultrasonic wave. The ultrasonic wave-front was incident on the specimen surface inclined to the vertical plane at an angle of either 18^{o} or 24^{o}. Since these angles lie between the first and the second critical angle, only vertically polarized shear waves propagated in the matrix and were incident on the fibre-matrix interface. Fig. 3a shows an SBR image from a fully consolidated single-fibre Ti-6Al-4V/SCS-6 composite. The same composite is imaged after the SFF test at ambient temperature. Fig. 3b clearly shows the fibre fractures of this composite system. Fig. 3c shows the ultrasonic image of a tensile tested single-fibre Ti-14Al-21Nb/SCS-6 composite at room temperature. The fibre fragments in this case are longer than in the case of a Ti-6Al-4V/SCS-6 composite.

The results were correlated with metallography. Fig. 4b shows the SEM micrograph of the Ti-6Al-4V/SCS-6 composite, ultrasonically imaged in Fig. 4a, after been subjected to tensile testing at room temperature. As it can be observed from comparing Figs. 4a and 4b, the SBR technique is adequate for evaluating in-situ fibre fragmentation characteristics in composites, including those with opaque matrix materials, such as metallic alloys.

From the characterization of the tested specimens, it became evident that the number of fragments increased with the increasing of fibre-matrix reaction. The distribution of fragment lengths measured for both composite systems, Ti-6Al-4V/SCS-6 and Ti-14Al-21Nb/SCS-6, fabricated by the two-stage process is presented in Fig. 5.

Tensile stress-strain curves for Ti-6Al-4V/SCS-6 and

Ti-14Al-2lNb/SCS-6 single fibre composites fabricated by the two-stage process, tested at 650°C, exhibited less amount of fragments compared to fragmentation tests performed at ambient temperatures. This can be explained by the fact that, when the fibre fragmentation test is performed at higher temperatures the relaxation of residual stresses dominates the fragmentation behaviour.

5. Estimation of Fibre/Matrix Interface Shear Strength

The interfacial shear strength refers to the maximum shear stress that can be transferred across the interface. Stress calculation at the interface can result in stress values exceeding the shear stress of the metal matrix, due to bonding and friction (roughness) at the interface. Thus, there is no apparent relationship between interfacial and metal matrix stress.

Based on the Kelly-Tyson model, if one measures the breaking strength of the fibre, one can estimate an effective interfacial strength τ_y from the critical fragment length L_c. When a specimen containing a single fibre is subjected to tensile deformation and the plastic matrix deforms beyond the elongation-to-break of the fibre, the fibre will break at its weakest point. At this point one has two pieces of fibre of different lengths. Under continued deformation, the fibre stress continues to increase until it reaches the breaking stress of one of the two fragments, at which point a second fracture occurs. This process will continue until all of the fragments are smaller than their critical lengths, after which fibre fracture is no longer possible. When a fibre of length L_c is fractured, two pieces of length $L_c/2$ should be obtained. The Kelly-Tyson model predicts that the fibre fracture process should result in a distribution of fragment lengths from $L_c/2$ to L_c. If the tensile strength of the fibre is independent of fibre length, one may calculate an effective interfacial shear strength τ_y from the measured critical length, using equation (1). Often, the distribution of fragment lengths obtained is broader than the 2:1 ratio predicted by the Kelly-Tyson model. This has been attributed to the variation of breaking strength with fibre length [33].

An estimate of an "effective" interfacial strength, τi, may be obtained from the midpoint of the cumulative distribution curve (i.e., at P=0.5) where the experimental fragment length is approximately 75% of L_c [33]. Using equation (1), one may estimate a value of τi from the median critical length and the mean tensile strength at that length, σ_m :

$$\tau_i = \frac{3}{8}\frac{\sigma_f\, d}{\bar{L}_f} \qquad (2)$$

From equation (2), calculation of τ_t can be done based on measuring the critical fragment length. Since

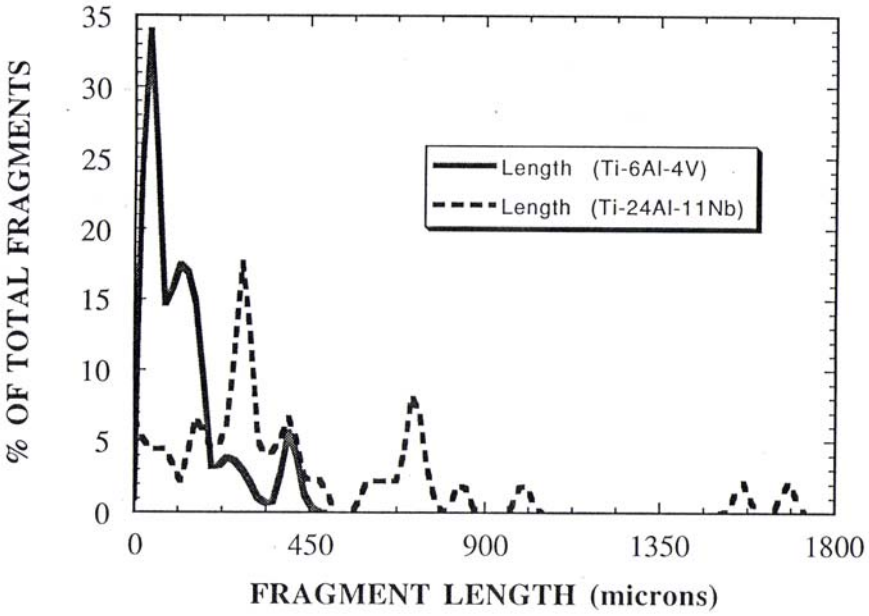

Fig. 5: Distribution of fragment lengths in Ti-6Al-4V/SCS-6 and Ti-14Al-21Nb/SCS-6 single fibre composites fabricated by the two-stage process, tensile tested at room temperature.

Table 2: Interfacial shear strength for the different composite systems.

COMPOSITES	τ_i (MPa) **RT tensile test**		τ_i (MPa) **HT tensile test**
	2-stage process	**1-stage process**	**2-stage process**
Ti-6Al-4V/SCS-6	989	277	136
Ti-14Al-21Nb/SCS-6	328	–	57

the fibre fragmentation test indicates the stress transfer behaviour from the matrix to the fibre, a stronger bond between fibre and matrix is expected to result in a shorter critical fragment length. The value of σ_f which is used in Kelly's equation is important for estimating the interfacial shear strength. The tensile strength of the fibre is assumed here to be $\sigma_f = 2600\ MPa$ [34], which was measured following fatigue loading of metal matrix composites and then extracting the bridging fibres. Such low values of fibre strength are also supported by the presence of flaws introduced by processing and shock wave, which weaken the fibre and give rise to low σ_f. In the literature, values of fibre strength as high as 4000 MPa have been reported. When the observed fragment lengths are employed in Kelly's equation using such high values of fibre strength, the obtained interfacial shear stresses are abnormally higher than the τ_i values obtained by push-out tests as well as those estimated from the matrix yield strength [35]. The diameter of SCS-6 fibre is d = 142 μm. The average fragment length for a Ti 6Al 4V/SCS 6 single fibre composite, fabricated by the two-stage process, tested at room temperature, is $\bar{L}_f = 0.14\ mm$, which leads (Eq. 2) to an estimated fibre/matrix interfacial shear strength of $\tau_i = 989\ MPa$. The average fragment length for a Ti 6Al 4V/SCS 6 single fibre composite, fabricated by the single-stage process, is $\bar{L}_f = 0.50\ mm$, which leads to an estimated fibre/matrix interfacial shear strength of $\tau_i = 277\ MPa$. The difference in interfacial shear strength between Ti 6Al 4V/SCS 6 composites fabricated by the two different routes can be explained in terms of processing. The excess reaction at interface in Ti 6Al 4V/SCS 6 specimens fabricated by the two-stage process leads to much higher values of τ_i. The average fragment length for a Ti 14Al 21Nb/SCS 6 single fibre composite fabricated by the two-stage process, which has less reaction at interface, is $\bar{L}_f = 0.422\ mm$, leading to an estimated fibre/matrix interfacial shear strength of $\tau_i = 328\ MPa$.

Based on the same analysis, the average fragment length for a Ti 6Al 4V/SCS 6 single fibre composite, fabricated by the two-stage process, tested at 650°C

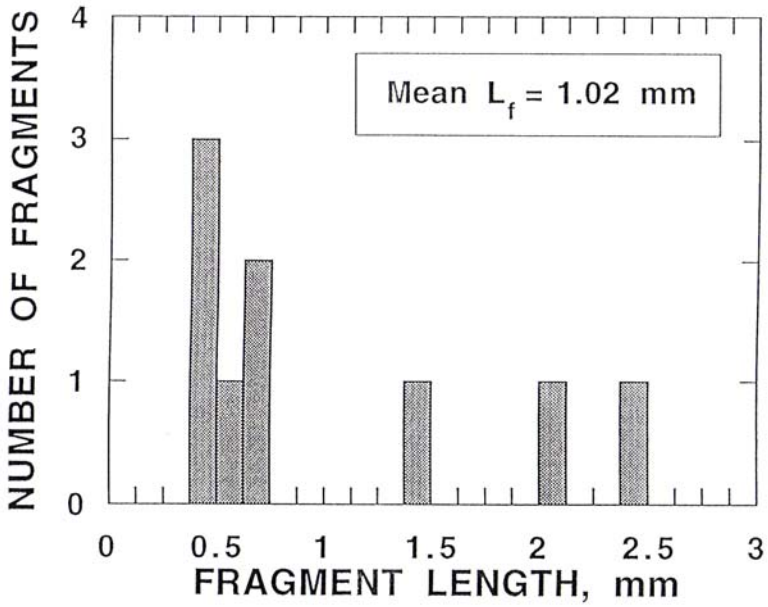

Fig. 6: Distribution of fragment lengths in Ti-6Al-4V/SCS-6 single fibre composite, fabricated by the two-stage process, tensile tested at 650°C.

was found to be $\bar{L}_f = 1.02\ mm$ (Fig. 6), leading to an estimated fibre/matrix interfacial shear strength of $\tau_i = 136\ MPa$. The average fragment length for a Ti 14Al 21Nb/SCS 6 single fibre composite, fabricated by the two-stage process, tested at 650°C was found to be $\bar{L}_f = 2.43\ mm$, leading to an estimated fibre/matrix interfacial shear strength of $\tau_i = 57\ MPa$. These values are low compared to the fibre/matrix interfacial shear strength of the same single fibre composite systems tested at room temperatures, due to relaxation of residual stresses. All results on interfacial shear strength are summarized in Table 2.

Reported in the literature values of interfacial shear strength for Ti-6Al-4V/SCS-6 are 295 MPa [36] and 180 MPa [37].

6. DETERMINATION OF THERMAL RESIDUAL STRESSES AT THE INTERFACE

Residual stresses are self-equilibrating internal stresses existing in a free body which has no external constraints acting on its boundary [38]. Residual stresses arise from the elastic response of the material to an inhomogeneous distribution of inelastic strains that arise due to plasticity, phase transformation, misfit, thermal expansion, etc. When the composite is fabricated at high temperatures both the fibre and the matrix are relatively stress-free and when they are cooled down to room temperature, residual stresses are introduced due to thermo-mechanical mismatch. This process-induced residual stress in composites is essentially thermal in nature, and is caused by a significant difference in the coefficients of thermal expansion of the fibre and the matrix and the large temperature differential of the cooling process.

If during the process of cooling the Von Mises stress exceeds yield stress at any temperature at a given point, then yielding occurs. It is to be noted that the thermal and mechanical properties of the constituents, Young's modulus, E, yield strength, σ_{YS}, flow modulus, H, and coefficient of thermal expansion, α, are all strong functions of temperature. Consideration of the thermal dependence of these properties is very important in the evaluation of the state of residual stress in this class of composites. In particular, the temperature dependence of CTE [39] of the two titanium matrix materials is shown in Fig. 7. The coefficients of linear thermal expansion for the temperature range 20°C – 900°C are 9.7 x 10-6 / °C and 9.9 x 10-6 / °C for Ti-6Al-4V and Ti-14Al-21Nb matrix materials, respectively. Further, the CTE of a 142 μm diameter SiC (SCS-6) monofilament has been determined to be 6.5 ± 0.5 X 10^{-6} / °C in the temperature range 25° – 900°C [40].

The micro-residual stresses in the composite are developed by a thermally induced linear strain mismatch ε_{th} between the matrix and the fibre,

$$\varepsilon_{th} = \Delta\alpha\ \Delta T \qquad (3)$$

where, $\Delta\alpha = \alpha_m - \alpha_f$ is the difference in linear thermal expansion coefficients for the composite constituents and $\Delta T = T - T_{ref}$ is the difference in temperature between the current state (ambient or testing temperature), T, and the reference temperature of the specimen at which the fibre is stress-free, T_{ref}. The state of stress at the peak temperature of the fabrication cycle can be assumed to be zero in the matrix and fibre [41], therefore Tref is the processing temperature of the composite. Table 3 summarizes the reference and testing temperatures in the present study.

In a fibre reinforced composite, the thermal residual stress, σr, at the fibre/matrix interface in the radial direction depends on the coefficient of thermal expansion mismatch, $\Delta\alpha = \alpha_m - \alpha_f$, between the matrix and fibre, and the effective temperature, ΔT, over which the residual stresses develop, and is given by [42]:

Table 3: Composite processing conditions and testing temperatures.

Processing Type	T (°C)	T_{ref} (°C) RT	T_{ref} (°C) HT
2-stage	985	23	650
1-stage	954	23	650

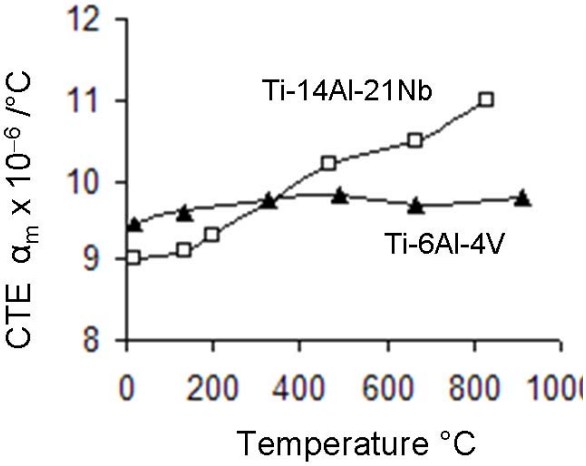

Fig. 7: Coefficients of thermal expansion of Ti-6Al-4V and Ti-11Al-21Nb alloys and the composite's processing cycle.

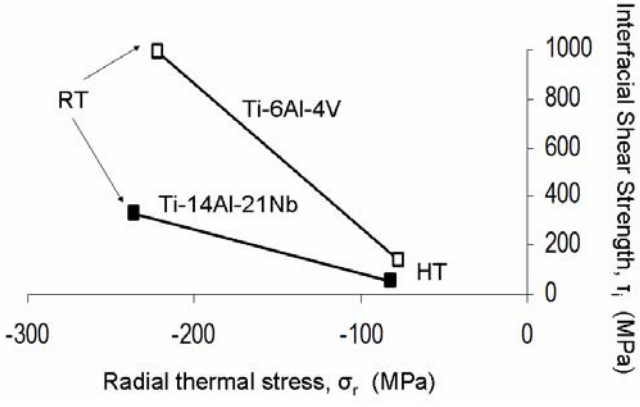

Fig. 8: Interfacial shear strength vs. radial thermal stress at the interface for two different composite systems, fabricated by the two-stage process and tensile tested at ambient and elevated temperatures.

$$\sigma_r = \frac{E_m E_f}{E_f(1+\nu_m) + E_m(1-\nu_f)}(\alpha_m - \alpha_f)(T - T_{ref}) \quad (4)$$

where E_m, E_f, ν_m and ν_f are the elastic moduli and Poisson's ratios of the matrix and the fibre, respectively.

The radial thermal stresses at the fibre/matrix interface (Table 4) were estimated based on Eq. 4) and taking into account Tables 1 and 3. These stresses are compressive.

The values of compressive radial thermal stress at the interface are in agreement with results reported in the literature. Coker, et. al. [43], for example, used a finite difference model to determine the three-dimensional stress state in a unidirectional composite subjected to axial, axisymmetric loading and changes in temperature. Their analysis accommodated multiple materials having elastic-plastic behaviour with strain hardening and a linearly elastic fibre. They assumed that the temperature distribution was uniform and quasi-static, and also a perfect bonding between the matrix and the fibre with no slippage or separation of the constituents. This model predicted for Ti-6Al-4V/SCS-6 composites a compressive stress of 400 MPa at the interface for a temperature difference between 925 °C and room temperature, and a compressive stress of 80 MPa for a temperature difference between 925 °C and 650 °C.

Fig. 8 depicts the influence of radial thermal micro-residual stresses on the interfacial shear strength. In this figure, the shear strength of the fibre/matrix interface is compared for two different composite systems (Ti-6Al-4V/SCS-6 and Ti-14Al-21Nb/SCS-6) fabricated using the same two-stage process. The microstructure of the interface region significantly differs in the two composite systems, as discussed above. The Ti 6Al 4V/SCS 6 composite system exhibited a significant reaction zone. In contrast, the Ti 14Al 11Nb/SCS 6 composite system showed a narrower and smoother interfacial reaction zone. As a result, the interfacial shear strength was expected to be much higher in the case of Ti 6Al 4V/SCS 6. At room temperature, this was indeed the case, and the difference in interfacial shear strength between the two composite systems was found to be

Table 4: Radial thermal residual stress at the fibre/matrix interface.

COMPOSITES	σ_r (MPa) **RT tensile test**		σ_r (MPa) **HT tensile test**	
	2-stage process	**1-stage process**	**2-stage process**	**1-stage process**
Ti-6Al-4V/SCS-6	-222	-215	-77	-70
Ti-14Al-21Nb/SCS-6	-236	-228	-82	-75

$\{\Delta\tau_i\}_{RT} = 661\ MPa$. However, the same difference at elevated temperature was found to be almost nine times lower, $\{\Delta\tau_i\}_{HT} = 79\ MPa$.

It should be pointed out that in a real composite the radial stresses should also be a function of fibre volume fraction. It is well known [44, 45] that the residual stresses in the matrix increase with the increasing volume fraction of fibres. Equation (4) which calculates the thermal stresses neglects the volume fraction. However, the values of radial stress at the interface shown for two composite systems, Ti-6Al-4V/SCS-6 and Ti-14Al-21Nb/SCS-6 in Table 4, would increase in a similar manner since the fibre material is the same in both cases. In this respect, Fig. 8, while is only valid for single fibre composites, will show a similar trend in the situation of high volume fraction composites, therefore, it is a valid representation of the comparative behaviour of the two composite systems.

7. CONCLUSIONS

The present work showed markedly different fibre fragmentation behaviour in Ti-6Al-4V/SCS-6 and Ti-14Al-2INb/SCS-6 single fibre composite samples arising from differences in the fibre/matrix interface. Fragmentation characteristics are significantly affected by fibre/matrix chemical reaction. Defects produced by this reaction at the fibre surface can lead to reduced fibre strength and result in extensive fragmentation of the fibre. This is influenced by matrix alloy composition as well as processing. This study has shown that the onset of fragmentation is related to the residual strain in the fibre. The influence of residual strain on the fragmentation behaviour is supported by results from fibre fragmentation testing done at higher temperatures.

Experiments at elevated temperature, supported by analytical modeling and ultrasonic imaging, indicated that shear stress transfer at the interface depends on several mechanisms, including residual stresses and chemical bonding. A comparison of the shear strength of the fibre/matrix interface for two different composite systems fabricated using the same two-stage process demonstrated that the interface load transfer behaviour largely depends on the thermal micro-residual stresses. At higher operating temperatures, where a release of radial compressive stresses clamping the fibre occur due to the small temperature differential between composite processing and operating/testing temperatures, the effect of interfacial reaction zone on the micro-mechanical properties of the composite is alleviated.

References:

1. **Reed, R.P. and Berg, J.C.,** "Measuring effective interfacial shear strength in carbon fibre bundle polymeric composites", *Journal of Adhesion Science and Technology*, **20**/160 (2006), 1929-1936.
2. **Torres, F.G. and Cubillas M.L.,** "Study of the interfacial properties of natural fibre reinforced polyethylene", *Polymer Testing*, **24**/60 (2005), 694-698.
3. **Kim, J.K. and Mai, Y.W.,** "Interfaces in composites in Structure and Properties of Fibre Composites", in Materials Science and Technology, Chou TW editor, VCH Publishers, Weinheim Germany, **13** (1993), 229-289.
4. **Kim, J.K., Zhou, L.M. and Mai Y.W.,** "Techniques for studying composite interfaces", in Handbook of Advanced Materials Testing, Cheremisinoff NP editor, Marcel Dekker, New York, chapter **22** (1994), 327-366.
5. **Zhou, L.M., Mai, Y.W., Ye, L. and Kim, J.K.,** "Techniques for evaluating interfacial properties of fibre-matrix composites", *Key Eng. Mater.*, **104-107** (1995), 549-600.
6. **Li, X.-M., Wang, J.-H., Gao, G.-Q. and Feng, W.,** "Study on the interfacial adhesion conditions by single-fibre composite fragmentation test", *Wuhan Ligong Daxue Xuebao/Journal of Wuhan University of Technology*, **27**/4 (2005), 9-12**.**
7. **Preuss, M., Rauchs, G., Withers, P.J., Maire, E. and Buffiere, J.-Y.,** "Interfacial shear strength of Ti/SiC fibre composites measured by synchrotron strain measurement", *Composites Part A: Applied Science and Manufacturing*, **33**/10 (2002), 1381-1385.
8. **Cox, H. L.,** "The elasticity and strength of paper and other fibrous materials", *J. Appl. Phys.*, **3** (1952), 73.
9. **Dow, N. F.,** "Study of stresses near a discontinuity in a filament-reinforced composite metal", in Space Sci. Lab. Missile and Space Div., General Electric Co. Tech., Report, No. R63SD61, 1963.
10. **Rosen, B. W.,** "Mechanics of composite strengthening", in Fibre Composite Materials, American Society of Metals, Metals Park, Ohio, (1964), 37.
11. **Amirbayat, J. and Hearle, W.S.,** "Properties of unit composites as determined by the properties of the interface. Part I: Mechanism of matrix-fibre load transfer", *Fibre Sci. Technol.*, 2 (1969), 123.
12. **Molliex, L., Favre, J.-P., Vassel, A. and Rabinovitch, M.,** "Interface Contribution to the SiC-

titanium and SiC-aluminium Tensile Strength Prediction", *J. Mater. Sci.*, **29** (1994), 6033-6040.

13. **Clough, R.B., Biancaniello, F.S., Wadley, H.N.G. and Kattner, U.R.,** "Fibre and Interface Fracture in Single Crystal Aluminum/SiC Fibre Composites", *Met. Trans.*, **21A**/10 (1990), 2747-2757.
14. **Houpert, J.-L., Phoenix, S.L. and Raj, R.,** "Analysis of the Single-Fibre-Composite Test to Measure the Mechanical Properties of Metal-Ceramic Interfaces", *Acta Metall. Mater.*, **42**/12 (1994), 4177-4187.
15. **Kelly, A. and Tyson, W.R.,** "Tensile Properties of Fibre-reinforced Metals: Copper/Tungsten and Copper/Molybdenum", *J. Mech. Phys. Solids*, **13** (1965), 329-350.
16. **Favre, J.-P. and Jacques, D.,** "Stress Transfer in Carbon Fibre Model Composites", *J. Mater. Sci.*, **25** (1990), 1373-1380.
17. **Waterbury, M.C. and Drzal, L.T.,** "On the Determination of Fibre Strengths by In-Situ Fibre Strength Testing", *J. Comp. Tech. Res.*, **13**/1 (1991), 22-28.
18. **Narkis, M., Chen, E.J.H. and Pipes, R.B.,** "Review of Methods for Characterization of Interfacial Fibre-Matrix Interactions", *Polymer Composites*, **9**/4 (1988), 245-251.
19. **Henstenburg, R.B. and Phoenix, S.L.,** "Interfacial Shear Strength Studies Using the Single-Filament-Composite Test. Part II: A Probability Model and Monte Carlo Simulation", *Polymer Composites*, **10**/6 (1989), 389-408.
20. **Roman, I. and Aharonov, R.,** "Mechanical interrogation of interfaces in monofilament model composites of continuous SiC fibre-aluminum matrix", *Acta Metall. Mater.*, **40**/3 (1992), 477-485.
21. **Nimmer, R.P., Bankert, R.J., Russell, E.S., Smith, G.A. and Wright, P.K.,** "Micromechanical modeling of fibre/matrix interface in transversely loaded SiC/Ti-6-4 metal matrix composites", *J. Comp. Technology and Research*, **13**/1 (1991), 3.
22. **Daniel, I.M. and Durelli,** "Shrinkage stresses around rigid inclusions", *Exper. Mech.*, **2** (1962), 240-255.
23. **Schapery, R.A.,** "Thermal expansion coefficients of composite materials based on energy principles", *J. Composite Mater.*, **2** (1968), 380-404.
24. **Chapman, T.J., Gillespie, J.W. and Pipes, R.B.,** "Prediction of process-induced residual stresses in thermoplastic composites", *J. Composite Mater.*, **24** (1990), 616-643.
25. **Bowles, D.E. and Griffin, O.H.,** "Micromechanics analysis of space simulated thermal stresses in composites, part I: Theory and unidirectional laminates", *J. Reinforced Plast.*, **10** (1991), 504-521.
26. **Sideridis, E.,** "Thermal expansion coefficients of fibre composites defined by the concept of the interphase", *Composites Sci. Technol.*, **51** (1994), 301-317.
27. **Chen, L.-G., Lin, S.-J. and Chang, S.-Y.,** "Tensile properties and thermal expansion behaviours of continuous molybdenum fibre reinforced aluminum matrix composites", *Compos. Sci. Technol.*, **66** (2006), 1793-1802.
28. **Marloff, R.H. and Daniel, I.M.,** "Three dimensional photoelastic analysis of a fibre reinforced composite midel", *Exp. Mech.*, **9** (1969), 156-162.
29. **Koufopoulos, T. and Theocaris, P.S.,** "Shrinkage stresses in two-phase materials", *J. Composite Mater.*, **3** (1969), 308-320.
30. **Barnes, J.A., Simms, I.J., Farrow, G.J., Jackson. D., Wostenholm, G. and Yates, B.,** "Thermal expansion characteristics of PEEK composites", *J. Mater. Sci.*, **26** (1991), 2259-2271.
31. **Pickard, S.M., Miracle, D.B., Majumdar, B.S., Kendig, K.L., Rothenflue, L. and Coker, D.,** "Experimental study of residual fibre strains in Ti-15-3 continuous fibre composites", *Acta Met. et Mater.*, **43**/8 (1994), 3105-3112.
32. **Matikas, T.E. and Karpur, P.,** "Ultrasonic Reflectivity Technique for the Characterization of Fibre-Matrix Interface in Metal Matrix Composites", *J. Appl. Phys.*, **74**/1 (1993), 228-236.
33. **DiBenedetto, A.T.,** "Evaluation of fibre surface treatments in composite Materials", *Pure & AppL Chem.*, **57**/11 (1985), 1659-1665.
34. **Kantzos, P., Eldridge, J., Koss, D.A. and Ghosn, L.J.,** "The effect of fatigue loading on the interfacial shear properties of SCS-6/Ti-Based MMCs", in Proceedings of MRS Spring meeting, San Francisco, California, 26 April –1 May 1992.
35. **Roman, I., Krishnamurthy, S. and Miracle, D.B.,** "Fibre-Matrix Interfacial Behaviour in SiC-Titanium Alloy Composites", in Titanium 92 Science & Technology, Froes, F.H., Caplan, I., eds., The Minerals, Metals & Materials Society, 1993.
36. **Vassel, A., Merienne, M.C., Pautonnier, F., Molliex and L., Favre, J.-P.,** "A Method to Evaluate the Bonding between Fibre and Matrix in Ti-Base Composite", in Proceedings of the 6th World Conference on Titanium, Lacombe P, Tricot R, Beranger G, editors, (1988), 919-923.
37. **Le Petitcorps, Y., Pailler, R. and Naslain, R.,** "The Fibre/matrix Interfacial Shear Strength in Titanium Alloy Matrix Composites Reinforced by Silicon Carbide or Boron CVD Filaments", *Compos. Sci. Technol.*, 35 (1989), 207-214.
38. **Mura, T.,** "Micromechanics of Defects in Solids", Martnus Nijhoff Publishers, The Hague Netherlands, 1982.
39. **Chandra, N., Ananth, C.R. and Garmestani, H.,** "Micromechanical modeling of process-induced residual stresses in Ti-24Al-11Nb/SCS-6 composite", *Journal of Composites Technology and Research*, **16**/1 (1994), 37-46.
40. **Elkind, A., Barsoum, M. and Kangutkar, P.,** "Thermal Expansion of Silicon Carbide Monofilaments and Silicon Carbide–Borosilicate Composites", *J. Am. Ceram. Soc.*, **75**/10 (1992), 2871–2873.
41. **Arnold, S.M., Ayra, V.K. and Melis, M.E.,** "Elastic/Plastic Analyses of Advanced Composites

Investigating the use of the Compliant layer Concept in Reducing Residual Stresses Resulting from Processing", NASA TM 103204, 1990.

42. **Jero, P.D., Kerans, R.J. and Parthasarathy, T.A,** "Effect of Interfacial Roughness on the Frictional Stress Measured using Pushout Tests", *J. Am. Ceram. Soc.*, **74**/11 (1991), 2793-2801.
43. **Coker, D., Ashbaugh, N.E. and Nicholas, T.,** "Analysis of thermomechanical cyclic behaviour of unidirectional metal matrix composites", in ASTM STP 1186, Sehitoglu H, editor, (1993), 50-69.
44. **Daehn, G.S., Anderson, P.M. and Zhang, H.,** "On the relationship between morphology and the resistance to temperature induced plasticity in reinforced composites", *Scripta Metallurgica et Materialia*, **25** (1991), 2285-90.
45. **Ho, S. and Lavernia, E.J.,** "Thermal Residual Stresses in Metal Matrix Composites: A Review", *Applied Composite Materials*, **2** (1995), 1-30.